Genetic Control Models with Diffusion and Delays*

JOSEPH M. MAHAFFY
Department of Mathematical Sciences,
San Diego State University, San Diego, California 92182

Received 1 June 1987; revised 23 January 1988

ABSTRACT

A compartmental model of genetic control by repression is examined. The model includes spatial diffusion in the compartment representing the cytoplasm and time delays for transcription and translation. A stability analysis is discussed for a range of diffusivities and cell radii. Numerical studies illustrate the analytical results and suggest a potential mechanism for the triggering of cell division based on the cell size.

1. INTRODUCTION

An important event in the life cycle of a cell is mitosis, where the cell divides into two new daughter cells, each with roughly half the mass of the parent cell. One of the unsolved mysteries in biology is exactly what triggers the cell to undergo this dramatic process of division. As division occurs when the cells achieve a certain size, one might examine models where size causes a change in behavior of the model. Several studies recently have examined the effects of cell size. One class of models assumes that the cell has its own internal clock which determines the onset of cell division (e.g., [8, 10, 11]). Another model assumes the existence of a yet to be discovered biochemical controller (e.g., [1, 15, 18]). Probablistic models of Tyson and Hannsgen [16, 17], which examine cell size as the control for cell division, have correlated well with experimental data. The model presented in this paper relies only on a simple negative feedback mechanism and size.

The model presented below is a fairly simple case where the cell is divided into two interacting compartments formed from concentric spheres. As the cell size increases, the stability of the concentrations of certain chemical species can be shown to change. The chemical species considered in this model are two of the critical components for cellular control by repression: mRNA and repressor. The model for this negative feedback system is

*Presented at the Los Alamos Conference for Nonlinear Studies in Biomathematics and Medicine, May 1987. This work was supported in part by National Science Foundation grant #DMS-8603787.

©Elsevier Science Publishing Co., Inc., 1988

developed in Mahaffy and Pao [13]. In the inner compartment mRNA is produced at a rate which is a decreasing function of the concentration of the repressor. The repressor is produced in the second compartment at a rate proportional to the concentration of the mRNA. Delays are introduced to account in the time required for the processes of transcription and translation of the chemical species. For certain parameter values it can be shown that this simple model undergoes a change of stability from stable to unstable as the size of the cell increases [5]. This implies that the chemical species change from maintaining a steady concentration to having oscillations in their concentrations. These epigenetic oscillations could provide the cell with a mechanism for triggering cell division.

From a mathematical point of view the model which is analyzed has some very interesting properties. The model is a system of reaction-diffusion equations with delays. A procedure is developed in Busenberg and Mahaffy [4, 5] which reduces this system of partial differential equations with delays to an equivalent system of delay differential equations and linear Volterra equations where the only spatial dependence occurs in an exponentially damped term containing the initial conditions. By linearizing the model and taking the limiting equations to damp out the dependence on the initial conditions, we are left with a system of equations which only depend on time. This system is analyzed using standard techniques for time varying systems. A method based on Mahaffy [12] is applied to the characteristic equation to determine for what parameter values the leading eigenvalues cross the imaginary axis, resulting in a loss of stability of the system.

2. FORMULATION OF THE MODEL

The biochemical basis of the model is a negative feedback system, repression, developed by Jacob and Monod [7]. Their model has been

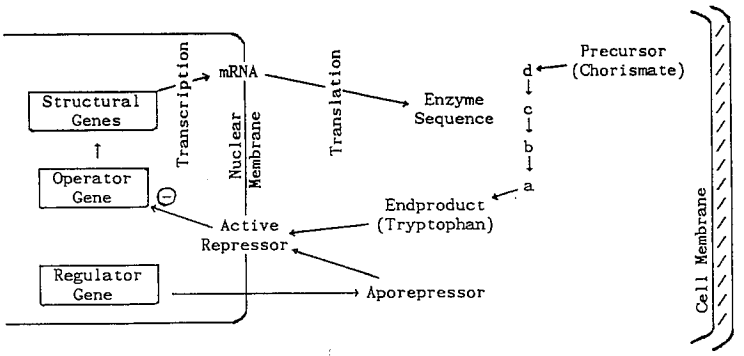

FIG. 1. Schematic for cellular control by repression.

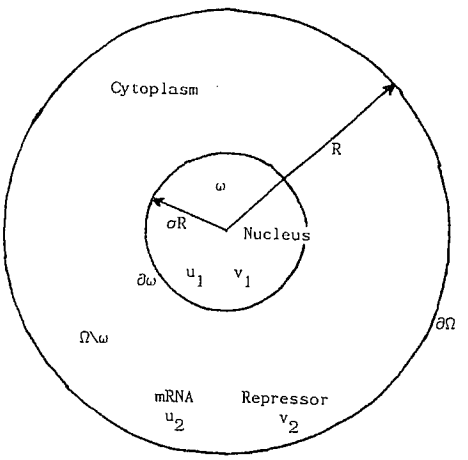

FIG. 2. Diagram for the compartmentalization of the cell.

substantiated for many biosynthetic pathways in prokaryotic cells, such as *E. coli*. Figure 1 shows a schematic representation for cellular control by repression using the biosynthesis of tryptophan as an example. Briefly stated, if the end product is in low supply, then the operator region of the gene is derepressed. This leads to transcription of the structural genes. This produces an mRNA which in turn is translated to form the end product or the enzymes necessary for the production of the end product. The end product then combines with an inactive repressor to produce an active repressor, which in turn binds to the operator region of the gene to prevent transcription of the structural genes. It is important to note that there are time delays for the processes of transcription and translation which should be considered in a model. The model is developed by assuming some substrates are in excess, certain equilibria are achieved instantaneously, and certain biochemical species are conserved. For a development of the mathematical model of this repression scheme the reader is referred to Banks and Mahaffy [2], Goodwin [6], or Othmer [14].

The model that will be considered in this article is an extension of the above idea which takes into account some of the physical attributes of the cell. Though there are ways of interpreting this model for a prokaryotic cell (simple bacterium), it will be discussed as if the cell were a eukaryote with a separate nucleus. The cell is physically divided into two compartments. (See Figure 2.) The first compartment is the nucleus, which is the smaller of the two compartments and as such will be considered well mixed. The second compartment is the cytoplasm, which allows diffusion. The nuclear membrane which separates the two compartments allows communication between

the compartments by passive diffusion. One assumes that all transcription occurs in the first compartment, ω, and that translation occurs only in the second compartment, $\Omega\backslash\omega$. If u_i and v_i, $i=1,2$, denote the concentrations of mRNA and repressor respectively in the two compartments, then combining the biochemical model with the physical compartmentalization, we obtain the following system of differential equations:

$$\begin{aligned}
\dot{u}_1(t) &= f(v_1(t-\nu_1)) - b_1 u_1(t) + \gamma_1 \int_{\partial\omega} [u_2(x,t) - u_1(t)]\, dS_\omega, \\
\dot{v}_1(t) &= -b_2 v_1(t) + \gamma_2 \int_{\partial\omega} [v_2(x,t) - v_1(t)]\, dS_\omega, \\
\frac{\partial u_2(x,t)}{\partial t} &= \mu_1 \nabla^2 u_2(x,t) - b_1 u_2(x,t), \\
\frac{\partial v_2(x,t)}{\partial t} &= \mu_2 \nabla^2 v_2(x,t) - b_2 v_2(x,t) + c_0 u_2(x,t-\nu_2), \qquad x \in \Omega\backslash\omega,
\end{aligned} \tag{2.1}$$

with boundary conditions

$$\begin{aligned}
\frac{\partial u_2(x,t)}{\partial n} &= -\beta_1 [u_2(x,t) - u_1(t)], \qquad x \in \partial\omega, \\
\frac{\partial v_2(x,t)}{\partial n} &= -\beta_1^* [v_2(x,t) - v_1(t)] \qquad x \in \partial\omega, \\
\frac{\partial u_2(x,t)}{\partial n} &= \frac{\partial v_2(x,t)}{\partial n} = 0, \qquad x \in \partial\Omega.
\end{aligned}$$

The constants b_i are the kinetic rates of decay, γ_i are the transfer rates between the compartments, and c_0 is the rate constant for production of the repressor. The function f is a positive, decreasing function in v_1 and is often of the form $1/\{1+k[v_1(t-\nu_1)]^\rho\}$. The constants ν_i represent the delays from transcription and translation. k is a kinetic constant, and ρ is the Hill coefficient of cooperativity. Details on the derivation of this model can be found in Mahaffy and Pao [13].

To continue the analysis of the model we examine the specific cases of one, two, and three dimensional models with symmetric geometries, such as concentric spheres in the three dimensional case. The cell radius is given by R, and the inner radius is given by σR for two and three dimensions. The occurrence of oscillations in the model (2.1) can be seen in the simulations on the one-dimensional model shown in Figure 3, where all the parameters are fixed except the time delay accounting for the transcription and translation. The simulations show the concentrations of the mRNA and repressor in each of the compartments. In each case the simulation was begun with all concentrations at equilibrium, except for the concentration of the mRNA in the first compartment, which was elevated. The two graphs on the left show damped oscillatory behavior for the delay below some critical value. The two

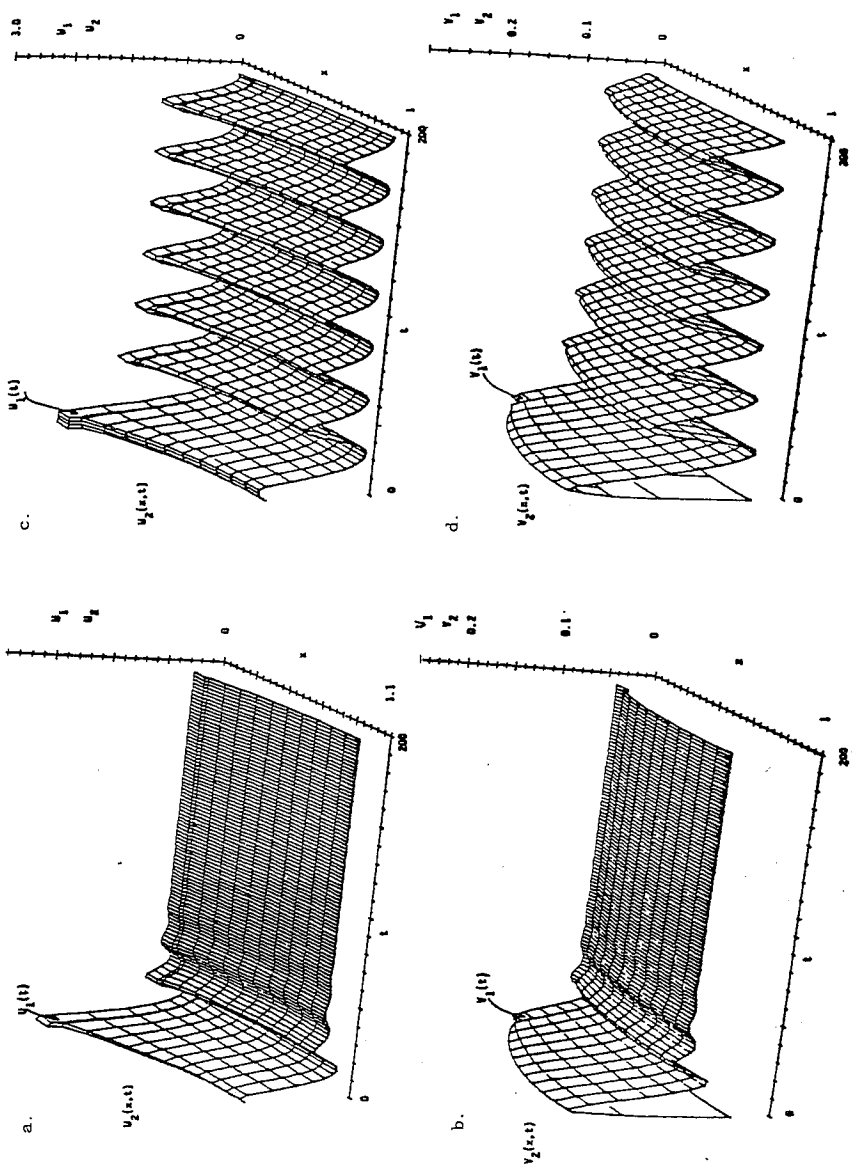

FIG. 3. Simulation of the model. (a) mRNA concentration for small delay. (b) Repressor concentration for small delay. (c) mRNA concentration for large delay. (d) Repressor concentration for large delay.

graphs on the right show that the model can sustain oscillations when the delay is above some critical value. We note that the behavior of the repressor, v, closely follows that of the mRNA, u.

3. MATHEMATICAL ANALYSIS OF THE MODEL

The simulations presented above suggest that there is a Hopf bifurcation for the reaction-diffusion model. To study this phenomenon in more detail, we make a change of variables which scales the time to eliminate b_1, translates the system to the equilibrium solution, and makes the boundary conditions homogeneous. Also, the radius of the cell is normalized so that $R=1$, and a translation in time for the u_i is made to shift the delays to the nonlinear term only. This results in the following set of equations:

$$\begin{aligned}
\dot{u}_1(\tau) &= f\big(v_1(\tau-\nu)+\bar{v}_1\big) - u_1(\tau) + \gamma_1 u_2(\sigma,\tau) + \gamma_1 u_2^s(\sigma) - (1+\gamma_1)\bar{u}_1 \\
&\equiv F_1\big(u_1(\tau), v_{1\tau}, u_2(\sigma,\tau)\big), \\
\dot{v}_1(\tau) &= -b_2 v_1(\tau) + \gamma_2 v_2(\sigma,\tau) \equiv G_1\big(v_1(\tau), v_2(\sigma,\tau)\big), \\
\frac{\partial u_2(r,\tau)}{\partial \tau} &= \mu_1 \nabla^2 u_2(r,\tau) - u_2(r,\tau) - u_1(\tau) - F_1\big(u_1(\tau), v_{1\tau}, u_2(\sigma,\tau)\big) \\
&\equiv \mu_1 \nabla^2 u_2(r,\tau) - u_2(r,\tau) - F_2\big(v_{1\tau}, u_2(\sigma,\tau)\big), \\
\frac{\partial v_2(r,\tau)}{\partial \tau} &= \mu_2 \nabla^2 v_2(r,\tau) - b_2\big[v_2(r,\tau)+v_1(\tau)\big] + c_0\big[u_2(r,\tau)+u_1(\tau)\big] \\
&\quad - G_1\big(v_1(\tau), v_2(\sigma,\tau)\big) \\
&\equiv \mu_2 \nabla^2 v_2(r,\tau) - b_2 v_2(r,\tau) - G_2\big(u_1, u_2(r,\tau), v_2(\sigma,\tau)\big),
\end{aligned} \tag{3.1}$$

with boundary conditions

$$\frac{\partial u_2(\sigma,\tau)}{\partial r} = \beta_1 u_2(\sigma,\tau), \qquad \frac{\partial v_2(\sigma,\tau)}{\partial r} = \beta_1^* v_2(\sigma,\tau),$$
$$\frac{\partial u_2(1,\tau)}{\partial r} = \frac{\partial v_2(1,\tau)}{\partial r} = 0,$$

where $v_{1\tau} = v_1(\tau-\nu)$ and the parameter ν is the dimensionless delay for the system. The other kinetic parameters are scaled appropriately; details of this change of variables are to be found in Busenberg and Mahaffy [5].

The above system of differential equations appears to be very complicated. However, on closer inspection we observe that the first two equations are delay-differential equations in u_1 and v_1 which in addition to their dependence on u_1 and v_1 depend on u_2 and v_2 on the boundary separating the two compartments. The third equation shows that the function F_2 depends only on u_2 along the boundary and v_1, which is only a time

dependent function. As this equation has homogeneous boundary conditions, we suspect that a variation of constants technique could be applied. We examine the linear part of the partial differential equation in u_2 and use separation of variables to find the eigenvalues and eigenfunctions, which are presented below for one, two, and three dimensions. The eigenvalues satisfy

$$\begin{aligned}
&\cot\lambda - \frac{\lambda}{\beta_1} = 0,\\
&\lambda\left[J_1(\lambda\sigma)Y_1(\lambda) - J_1(\lambda)Y_1(\lambda\sigma)\right]\\
&\qquad - \beta_1\left[J_1(\lambda)Y_0(\lambda\sigma) - J_0(\lambda\sigma)Y_1(\lambda)\right] = 0,\\
&(\lambda^2\sigma + 1)\sin\lambda(1-\sigma) - \lambda(1-\sigma)\cos\lambda(1-\sigma)\\
&\qquad - \beta_1\sigma\left[\lambda\cos\lambda(1-\sigma) - \sin\lambda(1-\sigma)\right] = 0.
\end{aligned} \tag{3.2}$$

The corresponding eigenfunctions $\phi_n(r)$ are given by

$$\begin{aligned}
\phi_n(r) &= \frac{2\sqrt{\lambda_n}\cos(\lambda_n r)}{\sqrt{2\lambda_n + \sin(2\lambda_n)}},\\
\phi_n(r) &= \frac{\pi\lambda_n\sqrt{2}\left[Y_1(\lambda_n)J_0(\lambda_n r) - J_1(\lambda_n)Y_0(\lambda_n r)\right]}{\left\{4 - \sigma^2\pi^2\left(\lambda_n^2 + \beta_1^2\right)\left[J_0(\lambda_n\sigma)Y_1(\lambda_n) - J_1(\lambda_n)Y_0(\lambda_n\sigma)\right]^2\right\}^{1/2}},\\
\phi_n(r) &= \frac{2\sqrt{\lambda_n}\left[\lambda_n\cos\lambda_n(1-r) - \sin\lambda_n(1-r)\right]}{r\left\{\left(\lambda_n^2+1\right)\left[2\lambda_n(1-\sigma)\right] - 2\lambda_n\right.}\\
&\qquad \left. + 2\lambda_n\cos 2\lambda_n(1-\sigma) + \left(\lambda_n^2 - 1\right)\sin 2\lambda_n(1-\sigma)\right\}^{1/2}
\end{aligned} \tag{3.3}$$

in one, two, and three dimensions respectively.

If we define the quantities $A_n = 1 + \lambda_n^2\mu_1$, $\delta_n = \langle\phi_n, 1\rangle$, and $\alpha_n = \langle u_{20}, \phi_n\rangle$, where $u_{20}(r) = u_2(r,0)$ and $\langle f, g\rangle = \int_\sigma^1 f(r)g(r)r^{k-1}\,dr$, k being the dimension of the problem, then we can apply the variation of constants formula to the u_2 equation in (3.1) and obtain

$$\begin{aligned}
u_2(r,\tau) &= \sum_{n=1}^{\infty}\alpha_n e^{-A_n\tau}\phi_n(r) - \int_0^\tau\sum_{n=1}^{\infty}\delta_n\phi_n(r)\,e^{-A_n(\tau-s)}F_2(s)\,ds\\
&\equiv \sum_{n=1}^{\infty}\alpha_n e^{-A_n\tau}\phi_n(r) - \int_0^\tau K(\tau-s,r)\left[\tilde{f}\left(v_1(s-\nu)\right) + \gamma_1 u_2(\sigma,s)\right]ds,
\end{aligned}$$

where $K(\tau,r) = \sum_{n=1}^{\infty}\delta_n\phi_n(r)e^{-A_n\tau}$ and $\tilde{f}(v_1(s-\nu)) = f(v_1(s-\nu) + \bar{v}_1) + \gamma_1 u_2^s(\sigma) - (1+\gamma_1)\bar{u}$.

We note that F_2 is only a function of s under the integral, so we integrate the above equation for u_2 along the boundary ω and obtain a linear

Volterra equation for u_2 on the boundary ω. In the radially symmetric cases that we are examining this reduces to the following:

$$u_2(\sigma,\tau) = \sum_{n=1}^{\infty} \alpha_n e^{-A_n\tau}\phi_n(\sigma) - \int_0^{\tau} K(\tau-s,\sigma)\left[\tilde{f}(v_1(s-\nu)) + \gamma_1 u_2(\sigma,s)\right] ds. \quad (3.4)$$

If we let ζ_n and $\psi_n(r)$ be the eigenvalues and eigenfunctions for the linear part of the v_2 equation and define $B_n = b_2 + \zeta_n\mu_2$, $\delta_n^* = \langle\psi_n, 1\rangle$, $\alpha_n^* = \langle v_{20}, \psi_n\rangle$, and $K^*(\tau, r) = \sum_{n=1}^{\infty}\delta_n^* e^{-B_n\tau}\psi_n(r)$, then the linear Volterra equation for v_2 can be found. As in the case of u_2, the equation for v_2 can be integrated along boundary of ω to give following expression:

$$v_2(\sigma,\tau) = \sum_{n=1}^{\infty} \alpha_n^* e^{-B_n\tau}\psi_n(\sigma) + \int_0^{\tau} K^*(\tau-s,\sigma)\left[c_0 u_1(s) - \gamma_2 v_2(\sigma,s)\right] ds + c_0\int_0^{\tau}\sum_{n=1}^{\infty} e^{-B_n(\tau-s)}\psi_n(\sigma)\left\langle u_2(\cdot,s), \psi_n(\cdot)\right\rangle ds. \quad (3.5)$$

We combine the first two equations in (3.1) along with (3.4) and (3.5) to form a system of delay differential equations and linear Volterra equations. This system only has a spatial component from the contribution of the initial conditions and reflected in the definitions of α_n and α_n^*. We linearize this system and form the limiting Volterra equations, which removes the dependence of the system on the initial conditions. The result is the following system of delay differential equations and linear Volterra equations which have no spatial dependence:

$$\dot{u}_1(\tau) = \tilde{f}'(\bar{v}_1)\, v_1(\tau-\nu) - u_1(\tau) + \gamma_1 u_2(\sigma,\tau),$$

$$\dot{v}_1(\tau) = -b_2 v_1(\tau) + \gamma_2 v_2(\sigma,\tau),$$

$$u_2(\sigma,\tau) = -\int_0^{\infty} K(\tau-s,\sigma)\left[\tilde{f}'(\bar{v}_1)\, v_1(s-\nu) + \gamma_1 u_2(\sigma,s)\right] ds,$$

$$v_2(\sigma,\tau) = \int_0^{\infty}\Bigg[K^*(\tau-s,\sigma)\left[c_0 u_1(s) - \gamma_2 v_2(\sigma,s)\right] - c_0\left[\tilde{f}'(\bar{v}_1)\, v_1(s-\nu) + \gamma_1 u_2(\sigma,s)\right]\sum_{n=1}^{\infty}\mathcal{K}_n(\tau-s)\Bigg] ds, \quad (3.6)$$

where $\mathcal{K}_n(s) = \psi_n(\sigma)\int_0^s e^{-B_n t}\langle K(s-t,\cdot), \psi_n(\cdot)\rangle\, dt$.

As (3.6) is only a time varying system, we can employ standard techniques to study its stability. The characteristic equation is formed by

expanding the appropriate determinant, which yields

$$(\lambda+1)(\lambda+b_2)\left(1+\gamma_1\int_0^\infty K(s,\sigma)\,e^{-\lambda s}\,ds\right)\left(1+\gamma_2\int_0^\infty K^*(s,\sigma)\,e^{-\lambda s}\,ds\right)$$
$$-c_0\gamma_2\tilde{f}'(\bar{v}_1)\,e^{-\lambda r}$$
$$\left[\int_0^\infty K^*(s,\sigma)\,e^{-\lambda s}\,ds-(\lambda+1)\int_0^\infty\sum_{n=1}^{\infty}\mathcal{K}_n(s)\,e^{-\lambda s}\,ds\right]=0. \quad (3.7)$$

With some algebraic manipulations and expansion of the integral kernels and by considering the case of $\beta_1=\beta_1^*$, we can write (3.7) as follows:

$$(\lambda+1)\left[\lambda+1+\lambda_1^2\mu_1+\gamma_1\delta_1\phi_1(\sigma)+\gamma_1\sum_{n=2}^{\infty}\frac{\delta_n\phi_n(\sigma)\left(\lambda+1+\lambda_1^2\mu_1\right)}{\lambda+1+\lambda_n^2\mu_1}\right]$$
$$\cdot(\lambda+b_2)\left[\lambda+b_2+\lambda_1^2\mu_2+\gamma_2\delta_1\phi_1(\sigma)+\gamma_2\sum_{n=2}^{\infty}\frac{\delta_n\phi_n(\sigma)\left(\lambda+b_2+\lambda_1^2\mu_2\right)}{\lambda+b_2+\lambda_n^2\mu_2}\right]$$
$$-c_0\gamma_2 f'(\bar{v}_1)\,e^{-\lambda\nu}\left[\lambda_1^2\mu_1\delta_1\phi_1(\sigma)\right.$$
$$\left.+\sum_{n=2}^{\infty}\frac{\delta_n\phi_n(\sigma)\lambda_n^2\mu_1\left(\lambda+1+\lambda_1^2\mu_1\right)\left(\lambda+b_2+\lambda_1^2\mu_2\right)}{\left(\lambda+1+\lambda_n^2\mu_1\right)\left(\lambda+b_2+\lambda_n^2\mu_2\right)}\right]=0. \quad (3.8)$$

This characteristic equation appears very complicated, but an extension of a technique developed by Mahaffy [12] allows us to determine numerically when the eigenvalues λ are purely imaginary and thus find where a Hopf bifurcation occurs.

Before presenting the numerical results of the Hopf bifurcation analysis, we compare the model given by (3.1) with a related model where the second compartment is well mixed. This model is given by

$$\begin{aligned}
\dot{u}_1(t) &= f(v_1(t-r))-u_1(t)+a_1\left[u_2(t)-u_1(t)\right],\\
\dot{v}_1(t) &= -b_2v_1(t)+a_2\left[v_2(t)-v_1(t)\right],\\
\dot{u}_2(t) &= -u_2(t)+a_3\left[u_1(t)-u_2(t)\right],\\
\dot{v}_2(t) &= c_0u_2(t)-b_2v_2(t)+a_4\left[v_1(t)-v_2(t)\right]. \quad (3.9)
\end{aligned}$$

Using standard methods we can find the characteristic equation for (3.9). It can be shown to have the following form:

$$(\lambda+1)(\lambda+b_2)(\lambda+1+a_1+a_3)(\lambda+b_2+a_2+a_4)$$
$$-c_0a_2a_3f'(\bar{v}_1)\,e^{-\lambda\nu}=0. \quad (3.10)$$

One would expect that in the case of high diffusivities μ_i the model given by (3.1) should have qualitative behavior similar to the well-mixed model

given by (3.9). This behavior should be reflected by the leading eigenvalues in the characteristic equations (3.8) and (3.10). What one shows is that when the diffusivities become large the infinite sums in (3.8) vanish and $\delta_1\phi_1(\sigma)$ tends to one, and then it is not hard to see the similarity of the two characteristic equations. The following theorem states this result:

THEOREM 3.1 (BUSENBERG AND MAHAFFY [5])

Assume that the nondimensional diffusivities μ_i *tend to infinity and* $\beta_1\mu_1$ *and* $\beta_1^*\mu_2$ *are finite. Consider* λ *such that* $\operatorname{Re}\lambda > \max\{-1, -b_2\}$. *Then, in the limit, the solutions* λ *which satisfy the characteristic equation* (3.8) *for the model* (3.1) *equal the solutions* λ *to the characteristic equation* (3.10) *for the well-mixed two compartment model with* $\gamma_1 = a_1$, $\gamma_2 = a_2$, $\beta_1\mu_1 = a_3$, *and* $\beta_1^*\mu_2 = a_4$.

At the other extreme when the diffusivities are small, we find that there is a region of asymptotic stability. Physically, this can be explained by the concept that the chemical species cannot diffuse far enough into the second compartment to react before they break down. A theorem by Busenberg and Mahaffy [5] proves the existence of this stable region and is given below:

THEOREM 3.2

Suppose that $\beta_1\mu_1 = a_3$, $\beta_1^*\mu_2 = a_4$, *with* a_3, a_4 *fixed, and suppose that* μ_1, μ_2 *tend to zero. Then there exists* $d > 0$ *such that if* $0 < \mu_i < d$, *all solutions* λ *which satisfy the characteristic equation* (3.8) *have real parts less than zero.*

A result related to this theorem shows the effects of size. We would expect that as the size of the cell becomes large we would again see that the chemical species were not able to diffuse sufficiently far into the second compartment to react. This result is stated below in the following theorem of Busenberg and Mahaffy [5]:

THEOREM 3.3

For both the two and the three dimensional model with central symmetry, suppose that $\beta_1\mu_1 = a_3R$ *and* $\beta_1^*\mu_2 = a_4R$. *Then there exists a constant* $M > 0$ *such that if* $R > M$, *all solutions of the characteristic equation* (3.8) *have real parts less than zero.*

In the next section we demonstrate numerically that there is a region where the stability increases with decreasing R for the radius of the small cell.

4. NUMERICAL RESULTS AND DISCUSSION

In this section we discuss how to analyze the characteristic equations (3.8) and (3.10) and graphically display some of the results obtained by the

numerical scheme. At the end of this section we will discuss some interesting possibilities that are suggested from the stability analysis of the model given by (3.1). The technique for analysis of the characteristic equations that is employed is discussed in Mahaffy [12]. To begin we return to the well-mixed model (3.9). Its characteristic equation has the form

$$P(\lambda) + Q(\lambda)\, e^{-\lambda\nu} = 0, \tag{4.1}$$

where $Q(\lambda)$ is a constant. By considering the delay as the bifurcation parameter, the value of the delay where the eigenvalues cross the imaginary axis, a Hopf bifurcation, can be computed. The Hopf bifurcation is computed by finding an ω^* such that $|P(i\omega^*)| = |Q(i\omega^*)|$; then the critical delay ν_0 is found by the formula

$$\nu_0 = \frac{\pi + \arg Q(i\omega^*) - \arg P(i\omega^*)}{\omega^*}. \tag{4.2}$$

A theorem in Mahaffy [12] shows that this critical delay ν_0 is unique and that for all $\nu > \nu_0$, the system of differential equations (3.9) is unstable about its equilibrium solution. The method of proving this theorem uses the argument principle from complex variables, which is a geometric argument. This suggests that the technique will allow perturbations. As we have already noted in the high diffusivity case of Theorem 3.1, the characteristic equation (3.8) behaves as a perturbation of (3.10). With this in mind we can readily correlate the $P(\lambda)$ and $Q(\lambda)$ in (4.1) with the appropriate terms in (3.8). A bisection method is employed to find an ω^* such that $|P(i\omega^*)| = |Q(i\omega^*)|$, and then (4.2) is used to compute the critical delay for the characteristic equation (3.8).

Details of implementing this scheme required a Newton's method applied to (3.2), and then these eigenvalues were inserted into the eigenfunctions (3.3) which were used in (3.8). The sums were truncated when successive partial sums were "sufficiently small." The results for the stability analysis of (3.1) in one, two, and three dimensions for the critical delay versus the diffusivity are presented in Figure 4. In these computations the diffusivities are taken to be the same. In addition, the other kinetic constants are scaled appropriately so that the mass balance of the different dimensions agrees with the well-mixed model for a fixed volume ratio of 1:25 for the first compartment to the second compartment.

There are ten parameters in the dimensionless model. We took $b_2 = 0.2$, representing a fivefold increase in stability of the repressor over the mRNA. Using the repression scheme of Bliss et al. [3], we chose $\rho = 4$. The volume ratio for nucleus to cytoplasm ranged from 1:10 to 1:25, which is an acceptable biological range. We allowed transfer rates and diffusivities to be equal. No data were found to determine the kinetic constants β_1, c_0, and k.

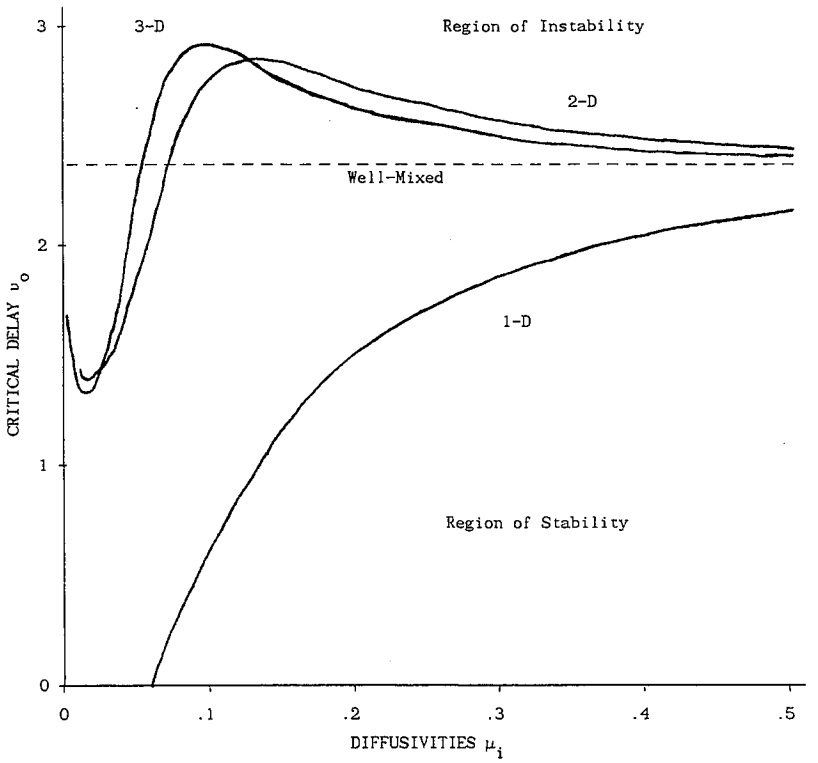

FIG. 4. Graph of the critical delay versus diffusivity.

The constant k was taken large to indicate a strong repression effect, while c_0 only affected relative concentrations and thus was unimportant in the stability analysis. The parameters for size, R, and diffusivity, μ_1, were examined over a wide range. Choice of these parameters is complicated by whether R should be increased to take account of the endoplasmic reticulum. Movement along the endoplasmic reticulum, unknown molecular weights, and other intracellular viscous effects complicate a choice of the diffusion constant. The simulations considered the known biological data; however, more studies are needed to determine the biological importance of the effects shown in the simulations.

Examining Figure 4, we see that the numerical results bear out the conclusions of Theorem 3.1. The results of Theorem 3.2 are only briefly observed with the upturn of the graphs in two and three dimensions for low diffusivities. This end of the graph is extremely time consuming to compute, as many terms in the infinite series are needed. The algorithm used to

compute the Bessel functions for the two dimensional case makes this case particularly time consuming. For intermediate values of the diffusivities we see some other interesting results. MacDonald [9] suggested that diffusion acts as a time delay and could be simply modeled as such. The characteristic equation (3.8) shows that diffusion acts in a more complicated manner than simply inserting a time delay. The numerical results for the one dimensional model do support MacDonald's argument, as there is a range of diffusivities where decreasing the diffusivities decreases the stability of the system. This is equivalent to adding a time delay. In fact, for a range of diffusivities below 0.06, the system becomes unstable without any delays in the equations. The graph does not consider diffusivity values sufficiently small for the effect of Theorem 3.2 to be seen in one dimension. However, in two and three dimensions the graphs are seen to show the opposite effect initially as the diffusivities are decreased. There is some local maximum value of the critical delay obtained before the graphs turn sharply downward and give the behavior of an additional delay. This behavior has not been explained to date and deserves further research.

Now we turn to the effects of size. By reintroducing the parameter R into (3.1) and showing how it affects the other kinetic parameters, we can readily perform calculations similar to the ones above, where instead of varying

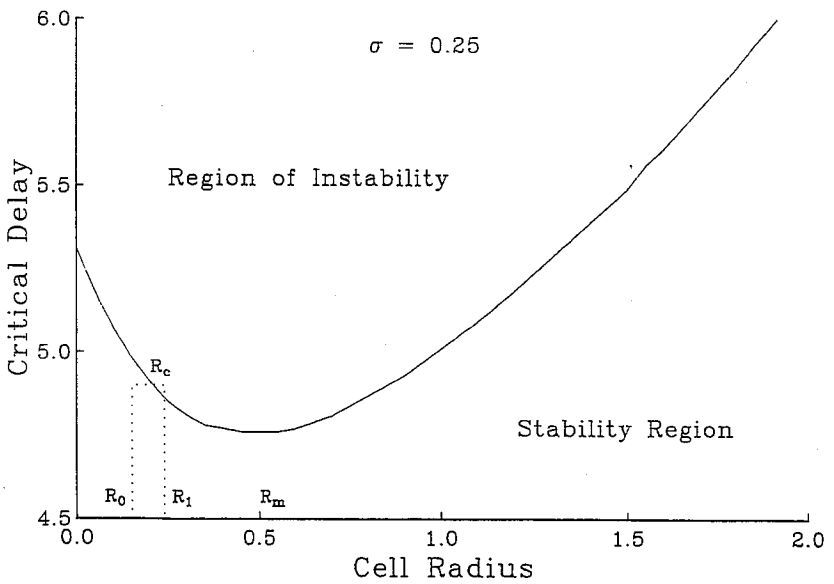

FIG. 5. Graph of the critical delay versus the cell radius R.

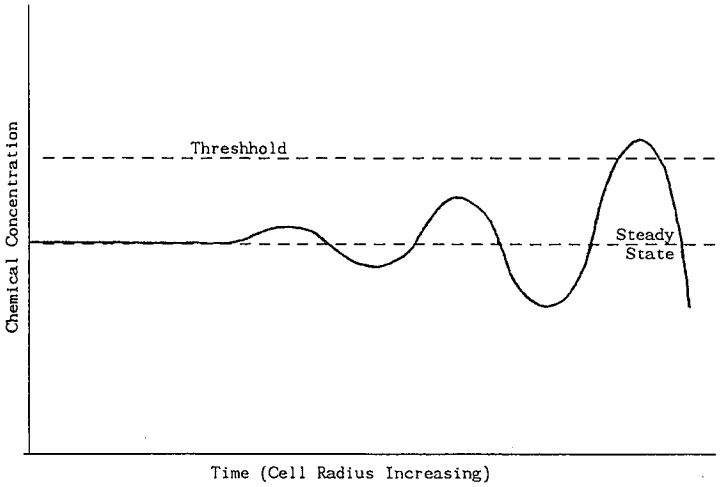

FIG. 6. Hypothesized triggering mechanism for a growing cell.

diffusivities we vary the radius R. A graph of the critical delay versus R is presented in Figure 5.

It is easy to see that the conclusion of Theorem 3.3 is demonstrated by the numerical results displayed in Figure 5. Numerically, there is one size R_m for which the concentrations of the chemical species are least stable. As the size of the cell increases above that size, the model becomes increasingly stable, until it is stable for all delays above $R = M$ for some M. Similarly, as the size decreases below R_m, the model becomes increasingly stable again, as stated in the comment following Theorem 3.3.

Next we show our hypothesized triggering mechanism. We consider that a newly divided cell has radius R_0 with delays for transcription and translation having a value of 4.9 as in Figure 5. At this point the cell is in a region of stability, which implies that the chemical concentrations remain constant. The chemical concentrations remain stable until the cell reaches a critical size R_c, where a Hopf bifurcation occurs. As the cell continues to grow, the oscillations of the chemical species become more pronounced until a critical size R_1 is achieved. At this point the cell divides and the cycle begins again. Figure 6 depicts this process. The horizontal axis represents time or increasing cell size, and the vertical axis shows the chemical concentration of our critical substance, the repressor. The actual triggering mechanism could use either a high or low threshhold value to signal cell division, or alternatively the cell could possess a gradient sensor which detects that the chemical concentration is oscillating. Whether this is the actual mechanism employed by a cell for division can be easily debated, but the mathematical phenome-

non of stability being lost with increasing size is interesting and certainly needs to be studied in more detail.

REFERENCES

1 W. Alt and J. J. Tyson, A stochastic model of cell division (with application to fission yeast), to appear.

2 H. T. Banks and J. M. Mahaffy, Mathematical Models of Protein Synthesis, Technical Report, Division of Applied Mathematics, Lefschetz Center for Dynamical Systems, Providence, R. I., 1979.

3 R. D. Bliss, P. R. Painter, and A. G. Marr, Role of feedback inhibition in stabilizing the classical operon, *J. Theoret. Biol.* 97:177–193 (1982).

4 S. N. Busenberg and J. M. Mahaffy, Interaction of spatial diffusion and delays in models of genetic control by repression, *J. Math. Biol.* 22:313–333 (1985).

5 S. N. Busenberg and J. M. Mahaffy, The effects of dimension and size of a compartmental model of repression, *SIAM J. Appl. Math.*, to appear.

6 B. C. Goodwin, Oscillatory behavior of enzymatic control processes, *Adv. Enzyme Reg.* 3:425–439 (1965).

7 F. Jacob and J. Monod, On the regulation of genome activity, *Cold Spring Harbor Symp. Quant. Biol.* 26:193–211, 389–401 (1961).

8 R. Klevecz, S. Kauffman, and R. Shymko, Cellular clocks and oscillators, *Internat. Rev. Cytol.* 86:97–128 (1984).

9 N. MacDonald, *Time Lag in Biological Models*, Lecture Notes in Biomathematics, Vol. 27, Springer, New York, 1978.

10 M. C. Mackey, A deterministic cell cycle model with transition probability behavior, in *Temporal Order* (L. Renzigand and N. I. Jaeger, Eds.), Springer, Berlin, 1985, pp. 315–320.

11 M. C. Mackey, M. Santavy, and P. Selepova, A mitotic oscillator with a strange attractor and distribution of cell cycle times, in *Nonlinear Oscillations in Biology and Chemistry* (H. Othmer, Ed.), Lecture Notes in Biomathematics, Vol. 66, Springer, Berlin, 1986, pp. 34–45.

12 J. M. Mahaffy, A test for stability of linear differential delay equations, *Quart. Appl. Math.* 40:193–202 (1982).

13 J. M. Mahaffy and C. V. Pao, Models of genetic control by repression with time delays and spatial effects, *J. Math. Biol.* 20:39–57 (1984).

14 H. G. Othmer, The qualitative dynamics of a class of biochemical control circuits, *J. Math. Biol.* 3:53–78 (1976).

15 J. J. Tyson and O. Diekmann, Sloppy size control of the cell division cycle, *J. Theoret. Biol.* 118:405–426 (1986).

16 J. J. Tyson and K. Hannsgen, The distribution of cell size and generation time in a model of the cell cycle incorporating size control and random transitions, *J. Theoret. Biol.* 113:29–66 (1985).

17 J. J. Tyson and K. B. Hannsgen, Global asymptotic stability of the size distribution in probabilistic models of the cell cycle, *J. Math. Biol.* 22:61–68 (1985).

18 J. J. Tyson and W. Sachsenmaier, The control of nuclear division in *Physarum polycephalum*, in *Cell Cycle Clocks* (L. N. Edwards, Jr., Ed.), Marcel Dekker, New York, 1984.